An equilibrium model for plate bending.*

B. Fraeijs de Veubeke †
and
G. Sander.††

Published in International Journal of Solids and Structures
Volume 4, pp. 447-468, 1968

Abstract.

A conforming displacement model for plate bending was presented earlier (5). It is of interest to have also an equilibrium model available in order to generate both upper and lower bounds to plate deflections. The theory of the triangular equilibrium model, which is presented here, is a revised version of that of reference 3, taking advantage of oblique coordinates. It is also extended to cover transverse loading modes. Because the numerical investigations required adaptability of the model to a stiffness computer-program, only the elaboration of the stiffness matrix was aimed at, following the general procedure set up in reference 2. The element can nevertheless be recognised as the Southwell analogue (4) of the plane stress model with quadratic displacement field described in reference 2. As such it could also be handled efficiently by a force program.
Numerical results show the expected monotonic convergence of deflections from above for the equilibrium model and from below for the conforming model. The convergence rate, in terms of total number of generalized coordinates, is compared with that of other plate bending elements.

* This research has been sponsored by the Air Force Flight Dynamics Laboratory under contract AF 6I(052)-892 through the European Office of Aerospace Research (EOAR), United States Air Force.

† Professor of Aerospace Engineering, University of Liège, Belgium.
†† Research assistant, Laboratoire de Techniques Aéronautiques et Spatiales, University of Liège, Belgium.

I. Plate equations in oblique coordinates.

The (x,y) axes of fig. I are taken to lie in the middle plane of the unstrained plate; the middle surface deflections $w(x,y)$ are taken positive upwards in the direction of Oz axis.

Bending an twisting moments are oriented by the right hand screw convention and correspond to oblique stress components positive in the upper layers. Shear loads are positively oriented as the transverse shear stresses.

We define covariant slopes of the middle surface by the formulas

$$\phi = -\frac{\partial w}{\partial x} = -w_{,x} \qquad \psi = -\frac{\partial w}{\partial y} = -w_{,y} \tag{I}$$

and verify that they are the orthogonal projections of the local rotation vector $\vec{\omega}$, lying in the middle plane, on the directions $\vec{k} \times \vec{i}$ and $\vec{k} \times \vec{j}$ respectively conjugate to $\vec{i}$ and $\vec{j}$. ($\vec{i}$, $\vec{j}$, $\vec{k}$) are unit vectors along the axes Ox, Oy and Oz respectively. Hence the conjugate direction to $\vec{i}$ is obtained by turning it of 90° about Oz in the positive (right-hand screw) sense. The same for the direction conjugate to $\vec{j}$ (fig. 2).

It is sufficient to carry out the proof for the $\vec{\omega}_o$ vector at the origin. In the neighborhood of the origin the rigid body displacement field is

$$\vec{w} = \vec{\omega} \times \vec{r}$$

where $$\vec{r} = x\,\vec{i} + y\,\vec{j}$$

Hence $$\vec{w} = (\vec{\omega} \times \vec{i})x + (\vec{\omega} \times \vec{j})y$$

$$= -(\vec{i} \times \vec{\omega})x - (\vec{j} \times \vec{\omega})y$$

In projection on the Oz axis

$$w = -x(\vec{i} \times \vec{\omega}).\vec{k} - y(\vec{j} \times \vec{\omega}).\vec{k}$$

and by definition (I) $\phi = (\vec{i} \times \vec{\omega}).\vec{k} = (\vec{k} \times \vec{i}).\vec{\omega}$

$$\psi = (\vec{j} \times \vec{\omega}).\vec{k} = (\vec{k} \times \vec{j}).\vec{\omega} \tag{2}$$

This property of covariant slopes is convenient because the bending and twisting moments are precisely oriented along the conjugate directions so that the virtual work of moments has a natural association with the covariant

components of rotation. For the elementary parallelogram of edges dx and dy the virtual work performed by moments in slope increases $\delta\phi$ and $\delta\psi$ is

$$\frac{\partial}{\partial x}(M_x\ \delta\phi + M_{xy}\ \delta\psi)dxdy + \frac{\partial}{\partial y}(M_{xy}\ \delta\phi + M_y\ \delta\psi)dxdy$$

The transverse shear loads Q_x and Q_y contribute

$$\frac{\partial}{\partial x}(Q_x\ \delta\ w)dxdy + \frac{\partial}{\partial y}(Q_y\ \delta\ w)dxdy$$

and the external transverse load distribution $q(x,y)$

$$q\ \delta\ w\ \sin\alpha\ dxdy$$

The total virtual work is stored as an increase in strain energy $\delta\ W\ \sin\alpha\ dxdy$, where W denotes the strain energy per unit area. Hence, after simplification by the common factor $dx\ dy$ and substitution of (I)

$$\sin\alpha\ \delta\ W = -\frac{\partial}{\partial x}\left(M_x\frac{\partial}{\partial x}\delta\ w + M_{xy}\frac{\partial}{\partial y}\delta\ w\right) - \frac{\partial}{\partial y}\left(M_{xy}\frac{\partial}{\partial x}\delta\ w + M_y\frac{\partial}{\partial y}\delta\ w\right)$$

$$+\frac{\partial}{\partial x}(Q_x\ \delta\ w) + \frac{\partial}{\partial y}(Q_y\ \delta\ w) + q\ \sin\alpha\ \delta\ w \qquad (3)$$

The equilibrium equations are now obtained by stating that there is no increase in strain energy when the additional deflection field is of rigid body type. Thus if δw = constant

$$\frac{\partial Q_x}{\partial x} + \frac{\partial Q_y}{\partial y} + q\ \sin\alpha = o \qquad (4)$$

If $\delta w = x \times$ constant

$$-\frac{\partial M_x}{\partial x} - \frac{\partial M_{xy}}{\partial y} + Q_x = o \qquad (5)$$

If $\delta w = y \times$ constant

$$-\frac{\partial M_{xy}}{\partial x} - \frac{\partial M_y}{\partial y} + Q_y = o \qquad (6)$$

Those equilibrium equations are formally identical with those in cartesian coordinates, only the factor $\sin \alpha$ in (4) betrays the obliquity of the axes. The general statement (3) can now be simplified by taking the equilibrium equations into account :

$$\sin \alpha \, \delta W = - M_x \, \delta w_{,xx} - 2 M_{xy} \, \delta w_{,xy} - M_y \, \delta w_{,yy} \qquad (7)$$

It shows that the strain energy per unit area is a function of the elements $(w_{,xx}, w_{,xy}, w_{,yy})$ of the curvature tensor such that

$$M_x = - \sin \alpha \, \frac{\partial W}{\partial w_{,xx}} \qquad 2 M_{xy} = - \sin \alpha \, \frac{\partial W}{\partial w_{,xy}} \qquad M_y = - \sin \alpha \, \frac{\partial W}{\partial w_{,yy}}$$

(8)

The complementary energy per unit area is defined, as usually, by the Legendre transformation

$$\Phi = w_{,xx} \frac{\partial W}{\partial w_{,xx}} + w_{,xy} \frac{\partial W}{\partial w_{,xy}} + w_{,yy} \frac{\partial W}{\partial w_{,yy}} - W$$

where the right hand side is to be expressed in terms of the conjugate variables M_x, M_{xy} and M_y. Differentiating totally

$$\Phi = - \frac{1}{\sin \alpha} (M_x w_{,xx} + 2 M_{xy} w_{,xy} + M_y w_{,yy}) - W \qquad (9)$$

and taking (7) into account

$$\delta \Phi = - \frac{1}{\sin \alpha} (w_{,xx} \, \delta M_x + 2 w_{,xy} \, \delta M_{xy} + w_{,yy} \, \delta M_y)$$

So that the dual energy relations are

$$w_{,xx} = - \sin \alpha \, \frac{\partial \Phi}{\partial M_x} \qquad 2 w_{,xy} = - \sin \alpha \, \frac{\partial \Phi}{\partial M_{xy}} \qquad w_{,yy} = - \sin \alpha \, \frac{\partial \Phi}{\partial M_y}$$

(10)

We know[1] that, for an isotropic plate of bending rigidity D, the strain energy density is

$$W = \frac{D}{\sin^2 \alpha}\left(\frac{1}{2} \theta_1^2 - (1 - \nu)\theta_2 \right) \tag{II}$$

$$\theta_1 = \frac{1}{\sin \alpha} (w_{,xx} + w_{,yy} - 2 \cos \alpha \; w_{,xy})$$

$$\theta_2 = w_{,xx} w_{,yy} - w_{,xy}^2$$

This gives by (8) the following curvature-moment relations

$$\sin^3\alpha \; M_x = - D\left(w_{,xx} - 2 \cos \alpha \; w_{,xy} + (\cos^2 \alpha + \nu \sin^2 \alpha) w_{,yy}\right)$$

$$\sin^3\alpha \; M_{xy} = - D \left(- \cos \alpha \; (w_{,xx} + w_{,yy}) + (1 + \cos^2 \alpha - \nu \sin^2 \alpha) w_{,xy}\right) \tag{I2}$$

$$\sin^3\alpha \; M_y = - D \left(w_{,yy} - 2 \cos \alpha \; w_{,xy} + (\cos^2 \alpha + \nu \sin^2 \alpha) w_{,xx}\right)$$

From this we find that

$$J_1 = M_x + M_y + 2 \cos \alpha \; M_{xy} = - D \; (1 + \nu) \; \theta_1$$

$$J_2 = M_x M_y - M_{xy}^2 = \frac{D^2}{\sin^2 \alpha} (\nu \; \theta_1^2 + (1 - \nu)^2 \theta_2) \tag{I3}$$

Solving for θ_1 and θ_2 and replacing into (II) which then becomes the complementary energy density

$$\Phi = \frac{1}{D(1 - \nu)} \left(\frac{1}{2(1+\nu)\sin^2 \alpha} J_1^2 - J_2 \right) \tag{I4}$$

The dual energy relations obtained from (I0) are then

$$D \; (1-\nu^2) \; w_{,xx} = - \frac{1}{\sin \alpha} (M_x + M_y + 2 \cos \alpha \; M_{xy}) + (1 + \nu) \sin \alpha \; M_y$$

$$D \; (1-\nu^2) \; w_{,xy} = - \frac{\cos \alpha}{\sin \alpha} (M_x + M_y + 2 \cos \alpha \; M_{xy}) - (1 + \nu) \sin \alpha \; M_{xy} \tag{I5}$$

$$D \; (1-\nu^2) \; w_{,yy} = - \frac{1}{\sin \alpha} (M_x + M_y + 2 \cos \alpha \; M_{xy}) + (1 + \nu) \sin \alpha \; M_x$$

2. Bending and twisting moments and Kirchhoff loads for arbitrary boundary orientation.

The analysis of an arbitrary triangular element is conveniently carried out by making two of the edges coincident with the oblique reference axes (fig. 3). The third edge is located by its intercepts a and b ; its length c is related to the lengths of the other edges by the elementary formula

$$c^2 = a^2 + b^2 - 2\,ab\cos\alpha$$

Other lengths which are convenient to introduce to simplify formulas are the two parts in which the third edge is cut by the perpendicular from o :

$$u = \frac{a(a - b\cos\alpha)}{c} \qquad v = \frac{b(b - a\cos\alpha)}{c} \qquad u + v = c \tag{I6}$$

In calculating the shear load Q_n , bending moment M_n and twisting moment M_{ns} corresponding to a facet of normal $\vec{n}$ in terms of Q_x , Q_y , M_x , M_{xy} and M_y at the same point, the lengths (a, b, c) are first considered as infinitesimals.

Then, since the contribution of the transverse load q is an infinitesimal of higher order, vertical equilibrium requires

$$c\,Q_n = b\,Q_x + a\,Q_y \tag{I7}$$

Again, in rotational equilibrium, the couples due to shear loads can be neglected as infinitesimals of higher order. Then, by considering equilibrium about an axis perpendicular to Ox

$$M_n\,b\sin\alpha - M_{ns}\,(a - b\cos\alpha) = b\,M_x + (a + b\cos\alpha)\,M_{xy} + a\cos\alpha\;M_y$$

and for equilibrium about Ox

$$M_n\,(a - b\cos\alpha) + M_{ns}\,b\sin\alpha = b\sin\alpha\;M_{xy} + a\sin\alpha\;M_y$$

These relations solved for M_n and M_{ns} can be written

$$M_n = \frac{\sin\alpha}{c^2}\,(b^2\,M_x + 2\,ab\,M_{xy} + a^2\,M_y) \tag{I8}$$

$$M_{ns} = -\frac{u}{a}\left(\frac{b}{c}\,M_x + \frac{a}{c}\,M_{xy}\right) + \frac{v}{b}\left(\frac{a}{c}\,M_y + \frac{b}{c}\,M_{xy}\right) \tag{I9}$$

Formulas (I7), (I8) and (I9) can now be applied to the third edge of the finite element, provided $(Q_x , Q_y , M_x , M_{xy} , M_y)$ are known along this edge. In particular, considering the virtual work equation

$$\int_1^2 (Q_n \, \delta w - M_{ns} \frac{\partial}{\partial s} \delta w) ds = - \left(M_{ns} \, \delta w\right)_1^2 + \int_1^2 (Q_n + \frac{\partial}{\partial s} M_{ns}) \delta w \; ds$$

it can be concluded that the shear stresses along this edge are statically equivalent to the Kirchhoff transverse load

$$K_{12} = Q_n + \frac{\partial}{\partial s} M_{ns} \tag{20}$$

and concentrated end loads (all defined positive upwards)

$$R_{12} = M_{ns} \quad \text{in} \quad 1$$

$$R_{21} = - M_{ns} \quad \text{in} \quad 2$$

Noting that along 12

$$\frac{\partial}{\partial s} = - \frac{a}{c} \frac{\partial}{\partial x} + \frac{b}{c} \frac{\partial}{\partial y}$$

substitution of (I7) and (I9) into (20) produces, after some transformations by the equilibrium equations (5) and (6)

$$K_{12} = 2 \frac{b}{c} Q_x + 2 \frac{a}{c} Q_y - \left(\frac{v}{b} \frac{\partial}{\partial x} + \frac{u}{a} \frac{\partial}{\partial y}\right) \left(\frac{b^2}{c^2} M_x + 2 \frac{a}{c} \frac{b}{c} M_{xy} + \frac{a^2}{c^2} M_y\right) \tag{2I}$$

while

$$R_{12} = - \frac{u}{a} \left(\frac{b}{c} M_x \, (a, o) + \frac{a}{c} M_{xy} \, (a, o)\right) + \frac{v}{b} \left(\frac{a}{c} M_y \, (a, o) + \frac{b}{c} M_{xy} \, (a, o)\right)$$

$$R_{21} = + \frac{u}{a} \left(\frac{b}{c} M_x \, (o, b) + \frac{a}{c} M_{xy} \, (o, b)\right) - \frac{v}{b} \left(\frac{a}{c} M_y \, (o, b) + \frac{b}{c} M_{xy} \, (o, b)\right)$$

If we let b tend to zero $(a \to c \, , \, u \to a \, , \, v/b \to - \cos \alpha)$ the formulas specialize to

$$M_n = \sin \alpha \; M_y \qquad (22)$$

$$y = o$$

$$M_{ns} = - M_{xy} - \cos \alpha \; M_y \qquad (23)$$

In this limiting process the material comes to lie on the wrong side of the edge $y = o$ of the finite element. For the material on the correct side, the analytical expressions remain invariant provided the positive orientations of M_n and M_{ns} are reversed, as indicated on figure 4 . However, in the case of the transverse loads we change signs in the limiting formulas in order to keep their definition as positive upwards. We then obtain along the edge $y = o$ of the finite element

$$K_{01} = - 2 Q_y - \cos \alpha \; \frac{\partial}{\partial x} M_y + \frac{\partial}{\partial y} M_y \qquad y = o \qquad (24)$$

$$R_{10} = M_{xy} (a, o) + \cos \alpha \; M_y (a, o)$$

$$R_{01} = - M_{xy} (o, o) - \cos \alpha \; M_y (o, o)$$

Similarly, by letting a tend to zero $(b \to c \; , \; v \to b \; , \; u/a \to - \cos \alpha)$ we find for the edge $x = o$

$$M_n = \sin \alpha \; M_x \qquad (25)$$

$$(x = o)$$

$$M_{ns} = \cos \alpha \; M_x + M_{xy} \qquad (26)$$

and the positive upwards transverse loads

$$K_{20} = - 2 Q_x - \cos \alpha \; \frac{\partial}{\partial y} M_x + \frac{\partial}{\partial x} M_x \qquad (x = o) \qquad (27)$$

$$R_{20} = \cos \alpha \; M_x (o, b) + M_{xy} (o, b)$$

$$R_{02} = - \cos \alpha \; M_x (o, o) - M_{xy} (o, o)$$

Combination of the concentrated loads at the corners produces the final corner loads

$$P_o = R_{01} + R_{02} = -2 M_{xy}(o, o) - \cos\alpha \,(M_x(o, o) + M_y(o, o))$$

$$P_1 = R_{12} + R_{10} = 2\frac{v}{c} M_{xy}(a, o) - \frac{b\,u}{a\,c} M_x(a, o) + \left(\cos\alpha + \frac{a\,v}{b\,c}\right) M_y(a, o) \qquad (28)$$

$$P_2 = R_{21} + R_{20} = 2\frac{u}{c} M_{xy}(o, b) - \frac{a\,v}{b\,c} M_y(o, b) + \left(\cos\alpha + \frac{b\,u}{a\,c}\right) M_x(o, b)$$

3. The linear field equilibrium model.

According to the general procedure for building up an equilibrium model [2], we start with an assumption concerning the stress field. It turns out that, if a 9 parameter linear bending-twisting moments field is adopted :

$$M_x = \beta_1 + \beta_2 \frac{x}{a} + \beta_3 \frac{y}{b}$$

$$M_{xy} = \beta_4 + \beta_5 \frac{x}{a} + \beta_6 \frac{y}{b} \qquad (29)$$

$$M_y = \beta_7 + \beta_8 \frac{x}{a} + \beta_9 \frac{y}{b}$$

the number of generalized loads required at the boundaries is exactly I2. These loads are connected by 3 overall equilibrium conditions reducing their degree of independance to 9 so that the model will be free of any spurious kinematical freedoms. The same conclusion is found directly if it is recognized that this plate equilibrium model is the Southwell analogue [3] of the quadratic displacement field triangular displacement model of reference 2. From (29), using equilibrium equations (5) and (6)

$$Q_x = \frac{1}{a}\beta_2 + \frac{1}{b}\beta_6 \qquad Q_y = \frac{1}{a}\beta_5 + \frac{1}{b}\beta_9 \qquad (30)$$

Equilibrium equation (4) shows then that the element will not accept a distributed transverse load q .

Methods for dealing with distributed transverse loads will be presented in a further section of the paper. The model will presently be restricted to accept only such external loads that conform with the interface distributions of stresses.

Equations (29) and (30) can now be substituted into (I8), (2I), (22), (24), (25), (27) and (28) to obtain the edge load distributions in terms of the stress parameters β_i .

For dimensional homogeneity all generalized loads will be defined as forces. The first 3 generalized loads will be the corner loads P_1 , P_2 and P_3 , their associated generalized displacements are obviously the local plate deflections w_1 , w_2 and w_3 at the corners. The next three generalized loads will be taken to be the total transverse forces due respectively to K_{01} , K_{12} and K_{20} . Noting that those Kirchhoff-type line loads are uniform we shall have

$$P_{01} = a\,K_{01} \qquad P_{12} = c\,K_{12} \qquad P_{20} = b\,K_{20} \tag{3I}$$

and, by virtual work considerations, their associated generalized displacements are the simple averages of plate deflections along the edges :

$$w_{01} = \frac{1}{a}\int_0^1 w\,dx \qquad w_{12} = \frac{1}{c}\int_1^2 w\,ds \qquad w_{20} = \frac{1}{b}\int_0^2 w\,dy \tag{32}$$

The last six generalized loads are due to the normal bending moments along the edges. They each have linear variations and are defined by two generalized quantities.

For instance along the edge 01 $(y = o)$

$$M_n = \sin\alpha\left(\beta_7 + \frac{x}{a}\,\beta_8\right)$$

This distribution is determined by the local values

$$\begin{aligned} M_{01} &= M_n\,(o,\,o) = \sin\alpha\;\beta_7 \\ M_{10} &= M_n\,(a,\,o) = \sin\alpha\;(\beta_7 + \beta_8) \end{aligned} \tag{33}$$

which are taken to be generalized loads. In terms of those

$$M_n = M_{01}\left(1 - \frac{x}{a}\right) + M_{10}\,\frac{x}{a} \tag{34}$$

The corresponding virtual work equation

$$\int_o^a M_n\;\phi\,dx = M_{01}\;\phi_{01} + M_{10}\;\phi_{10} \qquad \left(\phi = -\frac{\partial w}{\partial n}\right)$$

gives, after substitution of (34) and identification, the associated generalized displacements

$$\phi_{01} = a \int_o^1 \phi \left(1 - \frac{x}{a}\right) d\frac{x}{a} \qquad \phi_{10} = a \int_o^1 \phi \frac{x}{a} d\frac{x}{a} \tag{35}$$

In a similar fashion we define

$$M_{02} = \beta_1 \sin\alpha \qquad M_{20} = (\beta_1 + \beta_3) \sin\alpha \tag{36}$$

$$\phi_{02} = b \int_o^1 \phi \left(1 - \frac{y}{b}\right) d\frac{y}{b} \qquad \phi_{20} = b \int_o^1 \phi \frac{y}{b} d\frac{y}{b} \tag{37}$$

Along the edge 12 we set

$$\frac{x}{a} = \zeta \qquad \frac{y}{b} = 1 - \zeta \qquad o < \zeta < 1$$

so that, from (I8)

$$M_{12} = \frac{\sin\alpha}{c^2}\left(b^2 (\beta_1 + \beta_3) + 2\,ab\,(\beta_4 + \beta_6) + a^2 (\beta_7 + \beta_9)\right) \tag{38}$$

$$M_{21} = \frac{\sin\alpha}{c^2}\left(b^2 (\beta_1 + \beta_2) + 2\,ab\,(\beta_4 + \beta_5) + a^2 (\beta_7 + \beta_8)\right) \tag{39}$$

$$\phi_{12} = c \int_o^1 \phi (1 - \zeta)\, d\zeta \qquad \phi_{21} = c \int_o^1 \phi\, \zeta\, d\zeta \tag{40}$$

The result of expressing all generalized loads in terms of the stress parameters is summarized in the loads connection matrix C of table 1, where

$$g = C\,b \tag{4I}$$

$$g' = (P_o\ P_1\ P_2\ P_{01}\ P_{12}\ P_{20}\ M_{01}\ M_{10}\ M_{12}\ M_{21}\ M_{20}\ M_{02})$$

$$b' = (\beta_1\ \beta_2\ \beta_3\ \beta_4\ \beta_5\ \beta_6\ \beta_7\ \beta_8\ \beta_9)$$

The flexibility matrix F of the element results from

$$\iint \Phi \sin \alpha \, dx \, dy = \frac{1}{2} \beta' F \beta$$

where the complementary energy density (I4) is expressed through the invariants (I3) in terms of the stress parameters.
This flexibility matrix is presented in table 2 . It is to be inverted numerically to produce [2] the stiffness matrix K of the equilibrium model

$$g = K q \qquad K = C F^{-1} C'$$

$$q' = (w_1 \; w_2 \; w_3 \; w_{01} \; w_{12} \; w_{20} \; \phi_{01} \; \phi_{10} \; \phi_{12} \; \phi_{21} \; \phi_{20} \; \phi_{02})$$

4. Assembled stiffness matrices.

Some minor modifications to the direct stiffness method are required for assembling the individual stiffness matrices. All transverse loads and deflections are referred to a common positive upwards direction. Hence in the localizing matrix L_k of element (k)

$$q_{(k)} = L_k \, q$$

the first six rows are void except for a single unit in each, identifying a vertical displacement in the element with a nodal displacement of the structure.
However, bending moments and slopes at an interface have natural reference to reciprocal directions. This follows from the natural anticlockwise sense of definition of the bending moment orientations around each element (see fig. 4), or, alternatively, from the outward normal definitions of the conjugate slopes along the edges. As a consequence, in the six last rows of a localizing matrix, the units identifying a $\phi_{ij(k)}$ slope of element (k) with a nodal slope of the structure.will have to be affected by a sign. The sign will be positive if the nodal slope has same positive orientation, negative otherwise.
In some cases the mesh of elements and positive orientation of nodal slopes can be so devised that, for a given element, all positive slopes are codirectional with the nodal slopes (+ element) or antidirectional (- element).
A case in point is represented in fig. 5. The adjacent of a + element must then be a - element and this is obviously possible if the number of elements

meeting at an interior point remains even.

The nature of the external generalized loads that the structure can accept as an equilibrium model is also clear :

- at each vertex a concentrated transverse load can be associated with the local nodal deflection;
- along each interface segment, or boundary segment, a uniform transverse line load can be applied; its resultant is associated with the average deflection of the segment;
- each interface segment, or boundary segment, can be the axis of an applied couple of linearly varying intensity; the intensities at each end are the generalized external loads associated with the generalized slopes.

It should be noted that, just as the end intensities of the distributed couples have the physical dimensions of a force, the generalized slopes defined by (35, 36 or 40) have really the physical dimensions of a deflection.

5. Transverse surface loads.

From the viewpoint of equilibrium models the only correct way to introduce transverse surface loads is by increasing the number of generalized coordinates. Taking the simplest case, where the model is required to accept a uniform surface load q, let

$$p = \frac{1}{2} q \, ab \sin \alpha \tag{42}$$

the total load, be the additional generalized coordinate. The associated generalized displacement, obtained from virtual work consideration, is the ordinary average of deflection over the plate area

$$\bar{w} = \frac{2}{a\,b} \iint w \, dxdy \tag{43}$$

A particular field of bending and twisting moments and shear loads, satisfying the equilibrium equations (4), (5) and (6) under the uniform load is

$$\begin{aligned} M_x &= \frac{1}{3} p \; \frac{a}{b} \left(1 - \frac{x}{a}\right) \frac{x}{a} \\ M_{xy} &= -\frac{1}{3} p \; \frac{x}{a} \frac{y}{b} \\ M_y &= \frac{1}{3} p \; \frac{b}{a} \left(1 - \frac{y}{b}\right) \frac{y}{b} \end{aligned} \tag{44}$$

$$Q_x = \frac{p}{3\,b}\left(1 - 3\,\frac{x}{a}\right)$$

$$Q_y = \frac{p}{3\,a}\left(1 - 3\,\frac{y}{b}\right) \qquad (45)$$

It was derived from a general quadratic field in the bending and twisting moments by requiring

a) that the moments vanish along the three edges of the element

$$M_x = M_{xy} = o \qquad \text{for} \quad x = o$$

$$M_{xy} = M_y = o \qquad \text{for} \quad y = o$$

$$bM_x + aM_{xy} = o \qquad \text{and} \qquad aM_y + bM_{xy} = o \qquad \text{for} \quad \frac{x}{a} + \frac{y}{b} = 1$$

b) that the shear loads be constant along the edges

$$Q_x \quad \text{independant of} \quad y \quad \text{for} \quad x = o$$

$$Q_y \quad \text{independant of} \quad x \quad \text{for} \quad y = o$$

$$cQ_n = bQ_x + aQ_y \quad \text{constant for} \quad \frac{x}{a} + \frac{y}{b} = 1$$

The requirements are certainly sufficient to prevent the necessity of introducing new generalized interface loads. In fact the new external load p is simply reacted at the interfaces by three uniform Kirchhoff shear loads

$$K_x = -\frac{p}{3\,b} \qquad (-Q_x \quad \text{for} \quad x = o)$$

$$K_y = -\frac{p}{3\,a} \qquad (-Q_y \quad \text{for} \quad y = o)$$

$$K_n = -\frac{p}{3\,c} \qquad \left(\frac{b}{c}\,Q_x + \frac{a}{c}\,Q_y \quad \text{for} \quad \frac{x}{a} + \frac{y}{b} = 1\right)$$

The generalized reaction loads are, consequently

$$P_{01} = P_{12} = P_{20} = -\frac{1}{3}\,p \qquad (46)$$

$$P_0 = P_1 = P_2 = M_{01} = M_{10} = M_{12} = M_{21} = M_{20} = M_{02} = o \qquad (47)$$

The requirements a) and b) can in fact be regarded as necessary. For, if one allows the particular solution in equilibrium with a transverse pressure $q(x,y)$ to be reacted by a complete system of the (previously defined) generalized loads, superposition with a general field of type (29) can always implement the nine conditions (47) (equivalent to requirement a)) by adjustment of the nine β_i parameters.

If p is now considered to be the IOth stress parameter

$$p = \beta_{10} \tag{48}$$

equations (46) and (47) are incorporated in an augmented load connection matrix by bordering the C matrix of table I with a IOth column, hereafter written in transpose

$$(o \quad o \quad o \quad -1/3 \quad -1/3 \quad -1/3 \quad o \quad o \quad o \quad o \quad o \quad o).$$

Since p also becomes the I3th generalized load, C is further extended by a I3th border row

$$(o \quad o \quad o \quad o \quad o \quad o \quad o \quad o \quad o \quad 1)$$

expressing equation (48).

The flexibility matrix is also augmented and follows from computation of the strain energy as a quadratic form is the ten β_j parameters obtained by superposition of the fields (29) and (44) (where p is replaced by β_{10}). For an isotropic plate of constant rigidity D the elements of the additional column (and row) of the G matrix of table 2 turn out to be

$$\frac{1}{3}\left(\frac{a}{b} + \mu \frac{b}{a} - \cos\alpha\right)$$

$$\frac{1}{30}\left(4\left(\frac{a}{b} - \cos\alpha\right) + 3\mu\frac{b}{a}\right)$$

$$\frac{1}{30}\left(4\left(\mu\frac{b}{a} - \cos\alpha\right) + 3\frac{a}{b}\right)$$

$$\frac{2}{3}\left(\frac{a}{b} + \frac{b}{a}\right)\cos\alpha - \frac{1}{3}\lambda$$

$$\frac{1}{15}\left((4\,\frac{a}{b}+3\,\frac{b}{a})\cos\alpha-2\,\lambda\right)$$

$$\frac{1}{15}\left((3\,\frac{a}{b}+4\,\frac{b}{a})\cos\alpha-2\,\lambda\right)$$

$$\frac{1}{3}\left(\frac{b}{a}+\mu\,\frac{a}{b}-\cos\alpha\right)$$

$$\frac{1}{30}\left(4\,(\mu\,\frac{a}{b}-\cos\alpha)+3\,\frac{b}{a}\right)$$

$$\frac{1}{30}\left(4\,(\frac{b}{a}-\cos\alpha)+3\,\mu\,\frac{a}{b}\right)$$

$$\frac{2}{3}\left(\frac{a^2}{b^2}+\frac{b^2}{a^2}\right)-\frac{4}{3}\left(\frac{a}{b}+\frac{b}{a}\right)\cos\alpha+\frac{1}{9}\,(10\,\mu+4\,\lambda)$$

Clearly the process can be extended to cover more complicated surface load distributions. Even in the absence of surface loads, such extended models are valuable in that they yield additional information on the displacement field.

Should we wish to keep the simplicity of the original model and yet take surface loads $q(x,y)$ into account, one obvious procedure consists in replacing those surface loads by equivalent interface loads and rely on de Saint-Venant's principle to keep the effects of this substitution local. However the guarantee of upper deflection bounds is lost.

6. Numerical results.

In reference 7 a comprehensive numerical comparison was made between several models of plate bending elements under various loading and boundary conditions. Some of those results are again presented here in order to evaluate the performance obtained under similar conditions for the present equilibrium element and the conforming quadrilateral element of reference 5. Only those elements that exhibited satisfactory convergence characteristics were retained for comparison. In the code of reference 7 they are :

I. (ACM) a rectangular element developped by Adini, Clough and Melosh. It is based on a I2 parameter transverse displacement field, containing the complete cubic field (IO parameters) and, in addition, the x^3y and xy^3 terms. The generalized coordinates are the deflections and slopes at the 4 vertices. Continuity of the normal slope along the boundary is not secured, i.e. the element is not conforming.

2. (M) a rectangular element developped by Melosh on the basis of physical analogies with beam bending. It is a hybrid element, neither of the displacement nor of the equilibrium type.

3. (HCT) the so-called "high compatibility triangle" developped by Clough. It is a conforming model of the spline interpolation type. The major objective was to obtain a linear normal slope variation along each edge so that continuity of deflections and slopes could result from an identification of deflections and slopes at the vertices of the elements only.

4. (CQ) is our code name for the conforming quadrangular element, described earlier [5].

5. (EQT) is our code number for the present equilibrium triangle.

6. (Z) stands for a non conforming triangular displacement model developped by Bazeley, Cheung, Irons and Zienkiewicz [8]. This model was also used as the basis of conforming ones, pursuing a very similar objective to that of the HCT triangle. However this objective was reached differently. Inspection of the boundary conditions in areal coordinates permitted the addition of several types of correction fields, linearizing the normal slope variations. The conforming elements appear to be considerably stiffened and their convergence characteristics are difficult to assess from the numerical results reported.

The comparisons were performed for a square plate and a rectangular plate of aspect ratio 2, centrally loaded and with edges either clamped or simply supported. Symmetry allowed the treatment to be reduced to a quarter plate. The center deflections are reported in tables in the form of a dimensionless coefficient β defined by 3 to 6 (Fig.6)

$$w = \beta \frac{Pa^2}{D}$$

P : central load, a : size of quarter plate, D : bending rigidity.
The corresponding graphs (figs.7 to I0) are plots of

$$\mu = \frac{\beta_{computed} - \beta_{exact}}{\beta_{exact}}$$

The exact solution was computed by a Navier type series to the required four digit accuracy. The graphs are similar to those of reference 7 except that the new definition of the ordinate gives a direct estimate of percentage error and the use of the number of generalized coordinates in place of a mesh number provides a better comparison of accuracy versus computer load.

Convergence of deflections to their exact value is only one aspect of the accuracy of a computation. Convergence of the stress field is in many cases still more important. By their very nature, equilibrium models should be expected to yield better stress information than displacement models. A comparison is therefore included of the computed and exact bending moments along a symmetry axis for the simply supported square plate case. The test is severe since the exact bending moment tends to infinity as the central load is approached. Figure II illustrates the evolution of the bending moment distribution as the mesh size of the (CQ) element is reduced. Figure I2 illustrates the same for the (EQT) element. For clarity the exact distribution is not represented as it almost coincides with the computed solution with the finer mesh size. It is however represented in figure I3 where the performance of both models is compared for a given mesh size. The superiority of the equilibrium model in the large stress gradient region is thereby evidenced.

7. Conclusions.

Numerical results confirm the expected monotonic convergence characteristics of the central deflection from below for the conforming displacement elements (HCT and CQ) and from above for the equilibrium element (EQT). In particular the gap between the deflections of (EQT) and (CQ) constitutes a convenient quantitative estimator of the state of convergence. It is a good illustration of the general principle of a dual analysis in finite elements [6].

Non conforming and hybrid elements, such as (M) and (Z), can present excellent convergence rates, sometimes monotonic, sometimes oscillatory. However in problems where the exact solution is not accessible, the accuracy of computations based on such elements is more difficult to estimate since there is no guarantee of upper or lower bounds. The approximations based on the (CQ) element are, in most cases, the best, especially for crude idealizations; this is probably due to the additional freedom in normal slope variation along the edges. Suppressing this additional freedom by requiring a linear variation, as in the (HCT) triangle and conforming solutions based on the (Z) model, would probably make the element behave as (HCT) for a small number of generalized coordinates. The convergence characteristics of (EQT) are similar to those of (HCT) but from the other side. Furthermore (EQT) elements involve rapidly a high number of generalized displacements; as is generally the case with equilibrium elements it would be more efficiently handled by a Force computer program than by a Stiffness program.

Finally, both the (CQ) and the (EQT) element can provide an accurate representation of the stress field.

References.

I. L.S.D. MORLEY, Skew plates and structures, Pergamon, I963.

2. B. FRAEIJS de VEUBEKE, Displacement and equilibrium models in the finite element method. Chap. 9 of Stress Analysis, ed. O.C. Zienkiewicz and G.S. Holister, Wiley, I965.

3. G. SANDER, Bornes supérieures et inférieures dans l'analyse matricielle des plaques en flexion-torsion, Bull. Soc. R. Sci. Liège, V33, p. 456-94, I964.

4. B. FRAEIJS de VEUBEKE and O.C. ZIENKIEWICZ, Strain energy bounds in finite element analysis, by slab analogy. Journal of Strain Analysis, The Institution of Mechanical Engineers, London...

5. B. FRAEIJS de VEUBEKE, A conforming finite element for plate bending, International Journal of Solids and Structures.

6. G. SANDER and B. FRAEIJS de VEUBEKE, Upper and lower bounds to structural deformations by dual analysis in finite elements, Air Force Technical Report AFFDL-TR-I99, I966.

7. R.W. CLOUGH and J.L. TOCHER, Finite element stiffness matrices for analysis of plate bending, Proceedings of The Conference on Matrix Methods in Structural Mechanics, AFFDL-TR-66-80, I966, p. 5I5-546.

8. G.P. BAZELEY, Y.K. CHEUNG, B.M. IRONS and O.C. ZIENKIEWICZ, Triangular elements in plate bending - conforming and non-conforming solutions, Proceedings of The Conference on Matrix Methods in Structural Mechanics, AFFDL-TR-66-80, I966, p. 547-576.

List of captions.

Figure I. Stresses and moments in oblique coordinates

Figure 2. Definition of covariant slopes in oblique coordinates

Figure 3. Moments and shear load along slanting edge. Shear loads Q_x and Q_y are taken positive downwards , Q_n upwards.

Figure 4. Choice of positive orientations for interconnection (+ element).

Figure 5. A typical mesh of + type and - type elements.

Figure 6. Boundary conditions and idealization patterns of numerical calculations for centrally loaded plate.

Figure 7. Convergence curves of various types of finite elements. Square simply supported plate with central load.

Figure 8. Convergence curves. Square clamped plate with central load.

Figure 9. Convergence curves. Aspect ratio 2, simply supportes plate with central load.

Figure IO. Convergence curves. Aspect ratio 2, clamped plate with central load.

Figure II. Bending moment output of (CQ) model along y=0. Square simply supported plate.

Figure I2. Bending moment output of (EQT) model along y=0. Square simply supported plate.

Figure I3. Comparison of exact bending moment along y=0 and outputs of (CQ) and (EQT) models for given idealization patterns.

	β_1	β_2	β_3	β_4	β_5	β_6	β_7	β_8	β_9
P_o	$-\cos\alpha$	0	0	-2	0	0	$-\cos\alpha$	0	0
P_1	$-\frac{b}{a}\frac{u}{c}$	$-\frac{b}{a}\frac{u}{c}$	0	$2\frac{v}{c}$	$2\frac{v}{c}$	0	$\cos\alpha + \frac{a}{b}\frac{v}{c}$	$\cos\alpha + \frac{a}{b}\frac{v}{c}$	0
P_2	$\cos\alpha + \frac{b}{a}\frac{u}{c}$	0	$\cos\alpha + \frac{b}{a}\frac{u}{c}$	$2\frac{u}{c}$	0	$2\frac{u}{c}$	$-\frac{a}{b}\frac{v}{c}$	0	$-\frac{a}{b}\frac{v}{c}$
P_{01}	0	0	0	0	-2	0	0	$-\cos\alpha$	$-\frac{a}{b}$
P_{12}	0	$\frac{b}{a}(2-\frac{v}{c})$	$-\frac{b}{a}\frac{u}{c}$	0	$2\frac{u}{c}$	$2\frac{v}{c}$	0	$-\frac{a}{b}\frac{v}{c}$	$\frac{a}{b}(2-\frac{u}{c})$
P_{20}	0	$-\frac{b}{a}$	$-\cos\alpha$	0	0	-2	0	0	0
M_{01}	0	0	0	0	0	0	$\sin\alpha$	0	0
M_{10}	0	0	0	0	0	0	$\sin\alpha$	$\sin\alpha$	0
M_{12}	$\frac{b^2}{c^2}\sin\alpha$	0	$\frac{b^2}{c^2}\sin\alpha$	$\frac{2ab}{c^2}\sin\alpha$	0	$\frac{2ab}{c^2}\sin\alpha$	$\frac{a^2}{c^2}\sin\alpha$	0	$\frac{a^2}{c^2}\sin\alpha$
M_{21}	$\frac{b^2}{c^2}\sin\alpha$	$\frac{b^2}{c^2}\sin\alpha$	0	$\frac{2ab}{c^2}\sin\alpha$	$\frac{2ab}{c^2}\sin\alpha$	0	$\frac{a^2}{c^2}\sin\alpha$	$\frac{a^2}{c^2}\sin\alpha$	0
M_{20}	$\sin\alpha$	0	$\sin\alpha$	0	0	0	0	0	0
M_{02}	$\sin\alpha$	0	0	0	0	0	0	0	0

Table 2. The Flexibility Matrix of an isotropic element

$$F = \frac{a\ b}{I2(1-\nu^2)D\ \sin\alpha}\ G(\alpha,\nu)$$

$G(\alpha,\nu)$ is expressed below in terms of the auxiliary quantities

$$\lambda = 1 + \cos^2\alpha + \nu \sin^2\alpha$$

$$\mu = \cos^2\alpha - \nu \sin^2\alpha$$

6								
2	1							
2	0.5	1						
I2 cos α	4 cos α	4 cos α	I2 λ					
4 cos α	2 cos α	cos α	4 λ	2 λ				
4 cos α	cos α	2 cos α	4 λ	4 λ	2 λ			
6 μ	2 μ	2 μ	I2 cos α	4 cos α	4 cos α	6		
2 μ	μ	0.5 μ	4 cos α	2 cos α	cos α	2	1	
2 μ	0.5 μ	μ	4 cos α	cos α	2 cos α	2	0.5	1

Symmetrical

Table 3.

ANALYSIS	N = 1		N = 2		N = 4		N = 6		N = 8	
	N.G.C.	$\beta.10^3$	N.G.C.	$\beta.10$	N.G.C.	$\beta.10^3$	N.G.C.	$\beta.10^3$	N.G.C.	$\beta.10^3$
1 EXACT	—	II.6008	—	II.6008	—	II.6008	—	II.6008	—	II.6008
2 ACM	I2	I3.75	27	I2.30	75	II.8I	I47	II.69	273	II.64
3 M	I2	I2.I0	27	II.85	75	II.66	I47	II.6I	273	II.60
4 HCT	I2	8.84	27	I0.48	75	II.25	I47	II.44	273	II.48
5 CQ	I6	I0.876	39	II.439	II5	II.560	23I	II.588	—	—
6 EQT	I9	I3.770	57	I2.I24	I93	II.674	409	II.656	—	—
7 Z	I2	I3.02	27	II.76	75	II.65	I47	—	—	—

Case 1 : Square Plate - Simply Supported - Concentrated load in the center.

N.G.C. stands for Number of Generalized Coordinates

N is the mesh size number

β is defined by : $w_c = \beta \frac{Pa^2}{D}$

Table 4.

ANALYSIS	N = 1		N = 2		N = 4		N = 6		N = 8	
	N.G.C.	$\beta.10^3$	N.G.C.	$\beta.10^3$	N.G.C.	$\beta.10^3$	N.G.C.	$\beta.10^3$	N.G.C.	$\beta.10^3$
1 EXACT	—	I6.5239	—	I6.5239	—	I6.5239	—	I6.5239	—	I6.5239
2 ACM	I2	I8.487	27	I7.579	75	I6.9I9	I47	I6.745	273	I6.656
3 M	I2	I4.664	27	I6.476	75	I6.6I6	I47	I6.584	273	I6.570
4 HCT	I2	II.2I6	27	I3.60	75	I5.520	I47	I6.024	273	I6.24
5 CQ	I6	I4.486	39	I6.000	II5	I6.400	23I	I6.477	—	—
6 EQT	I9	22.I77	57	I7.878	I93	I6.804	409	I6.666	—	—

Case 2 : Rectangular Plate $(\frac{b}{a} = 2)$ - Simply Supported - Concentrated load in the center.

N.G.C. stands for Number of Generalized Coordinates

N is the mesh size number

β is defined by : $w_c = \beta \frac{Pa^2}{D}$

Table 5.

ANALYSIS	N = 1		N = 2		N = 4		N = 6		N = 8	
	N.G.C.	$\beta.10^3$	N.G.C.	$\beta.10^3$	N.G.C.	$\beta.10^3$	N.G.C.	$\beta.10^3$	N.G.C.	$\beta.10^3$
1 EXACT	—	5.605	—	5.605	—	5.605	—	5.605	—	5.605
2 ACM	I2	5.9I9	27	6.I37	75	5.807	I47	5.704	273	5.67I
3 M	I2	4.23I	27	5.736	75	5.688	I47	5.653	273	5.640
4 HCT	I2	I.O	27	4.2400	75	5.I92	I47	5.40	273	5.496
5 CQ	I6	5.208	39	5.430	II5	5.5708	23I	5.5966	—	—
6 EQT	I9	8.2565	57	6.I939	I93	5.7557	409	5.67I2	—	—
7 Z	I2	5.2I	27	5.89	75	5.72	I47	—	—	—

Case 3 : Square Plate - Clamped - Concentrated load in the center.

N.G.C. stands for Number of Generalized Coordinates

N is the mesh size number

β is defined by : $w_c = \beta \frac{Pa^2}{D}$

Table 6.

ANALYSIS	N = 1		N = 2		N = 4		N = 6		N = 8	
	N.G.C.	$\beta.10^3$	N.G.C.	$\beta.10^3$	N.G.C.	$\beta.10^3$	N.G.C.	$\beta.10^3$	N.G.C.	$\beta.10^3$
1 EXACT	—	7.2I5	—	7.2I5	—	7.2I5	—	7.2I5	—	7.2I5
2 ACM	I2	6.3923	27	7.799	75	7.5263	I47	7.3928	273	7.3342
3 M	I2	2.I8I5	27	6.7742	75	7.23I2	I47	7.2538	273	7.2490
4 HCT	I2	I.I56I	27	3.9546	75	6.I4I5	I47	6.6943	273	6.8384
5 CQ	I6	5.649	39	6.68I	II5	7.I06	23I	7.I798	—	—
6 EQT	I9	I3.937	57	8.7392	I93	7.5892	409	7.3786	—	—

Case 4 : Rectangular Plate ($\frac{b}{a} = 2$) - Clamped - Concentrated load in the center.

N.G.C. stands for Number of Generalized Coordinates

N is the mesh size number

β is defined by : $w_c = \beta \frac{Pa^2}{D}$

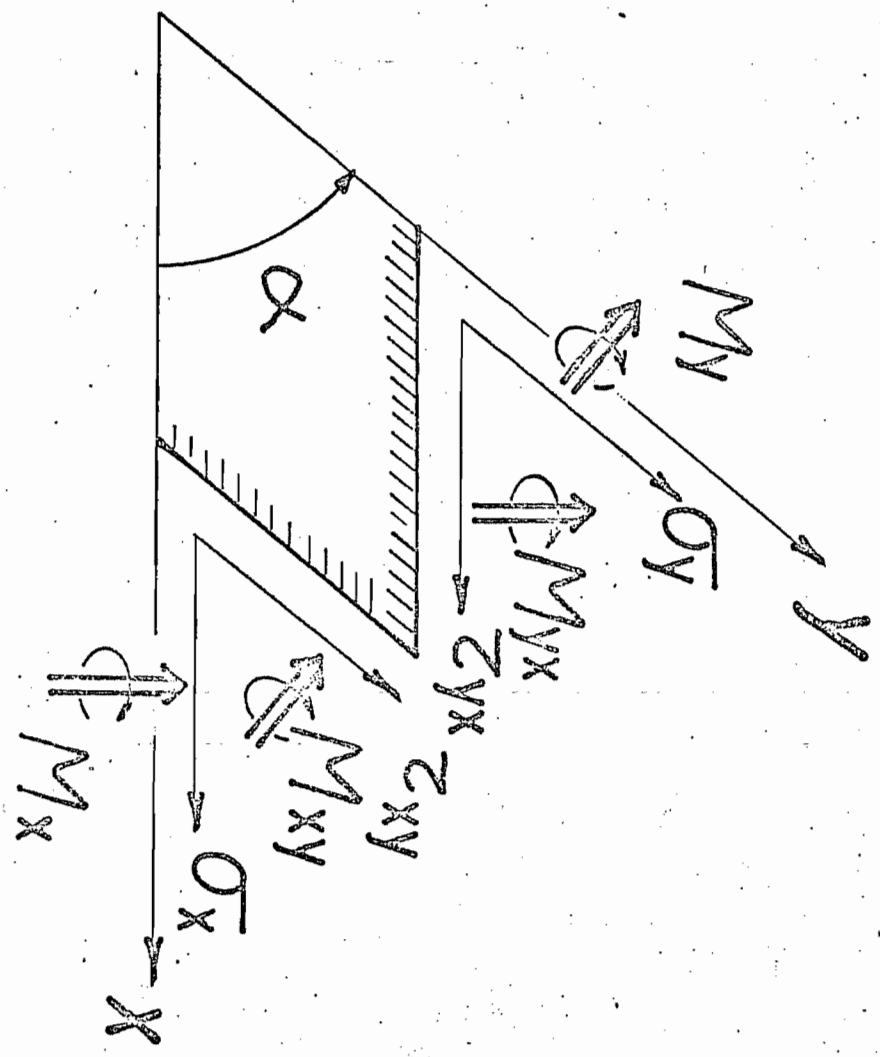

Figure I . Stresses and Moments in oblique coordinates.

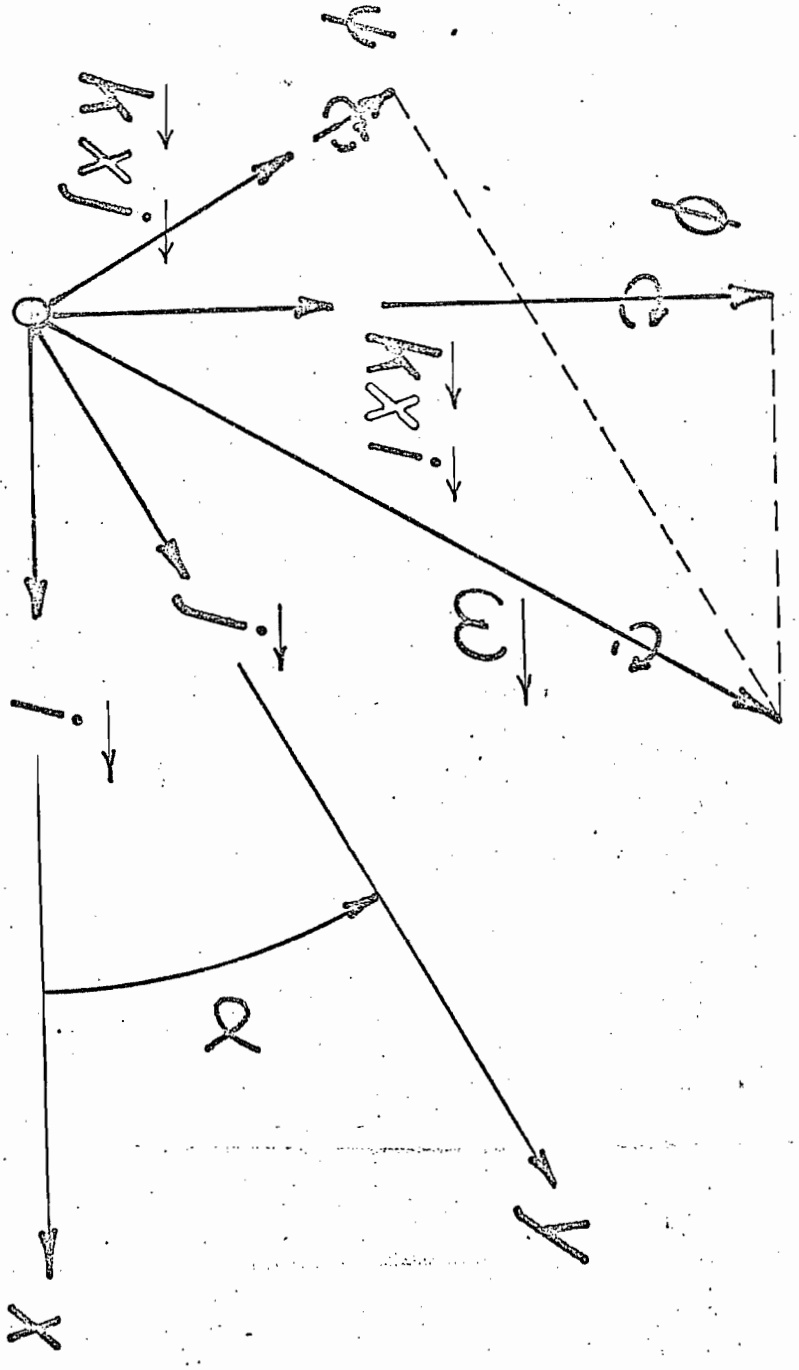

Figure 2. Definition of covariant slopes in oblique coordinates.

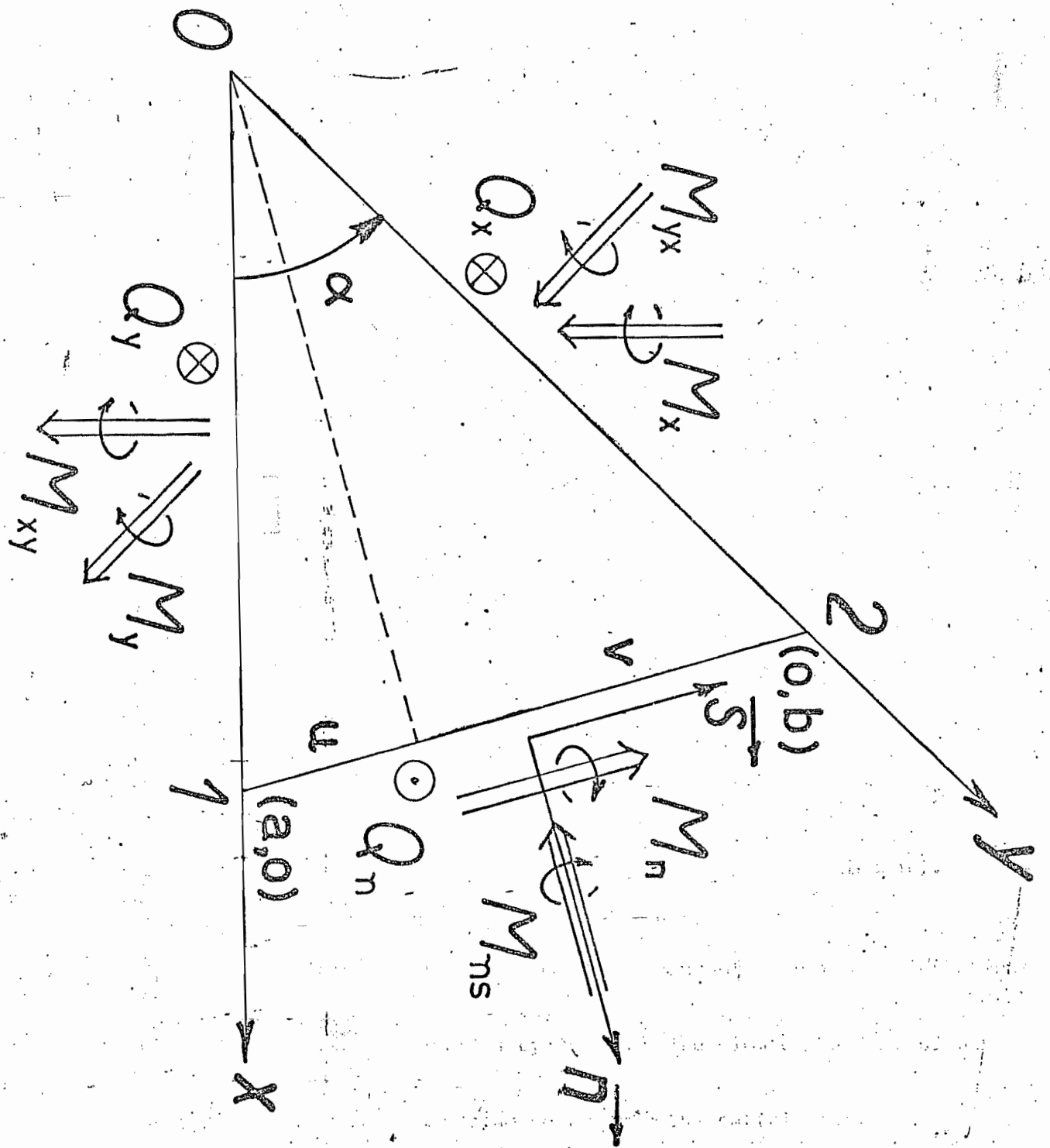

Figure 3. Moments and shear load along slanting edge. Shear loads Q_x and Q_y are taken positive downwards, Q_n upwards.

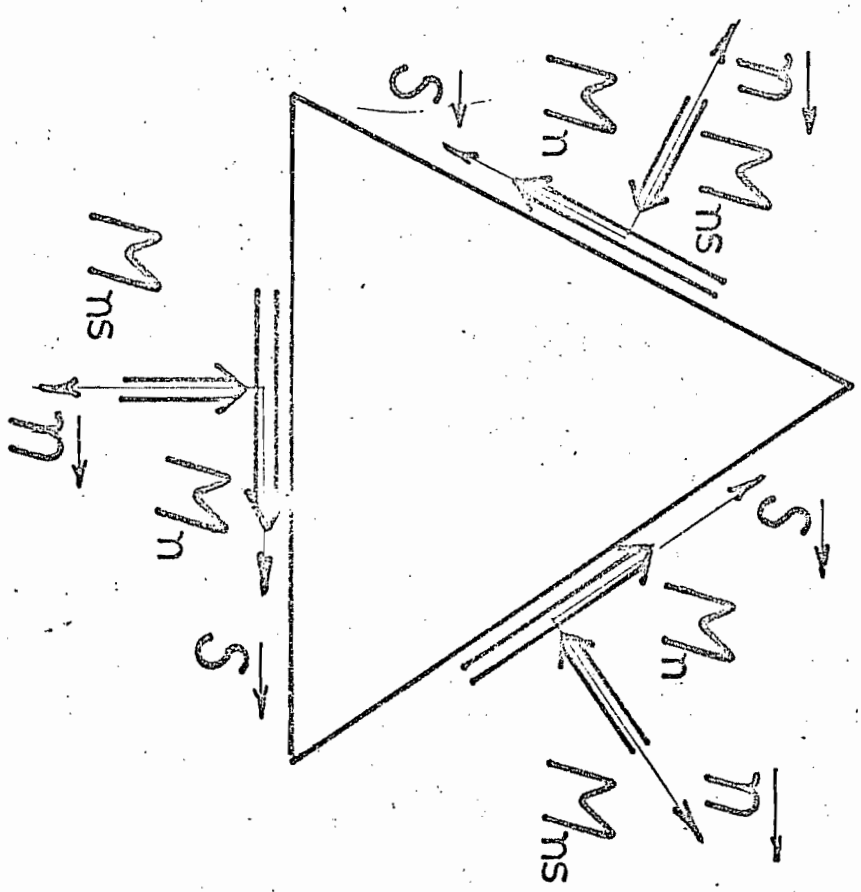

Figure 4. Choice of positive orientations for interconnection (+ element).

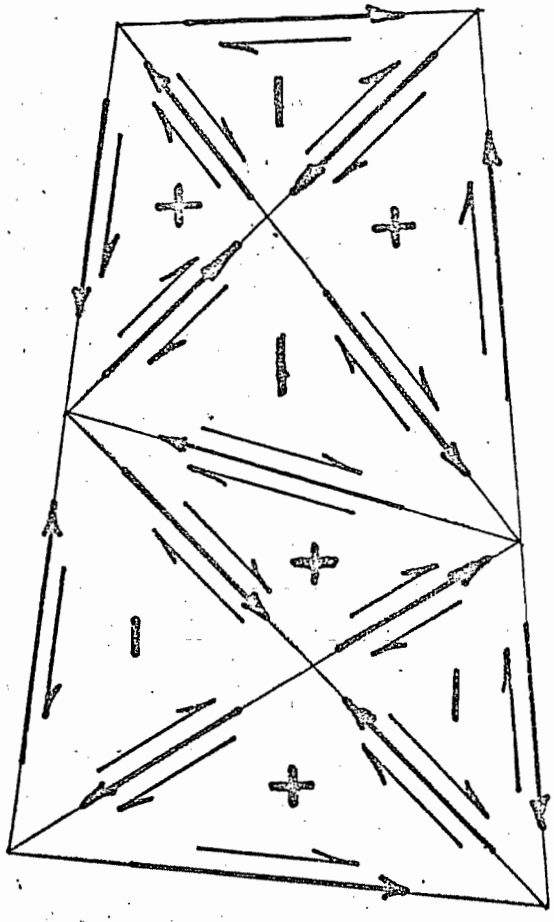

Figure 5. A typical mesh of + type and - type elements.

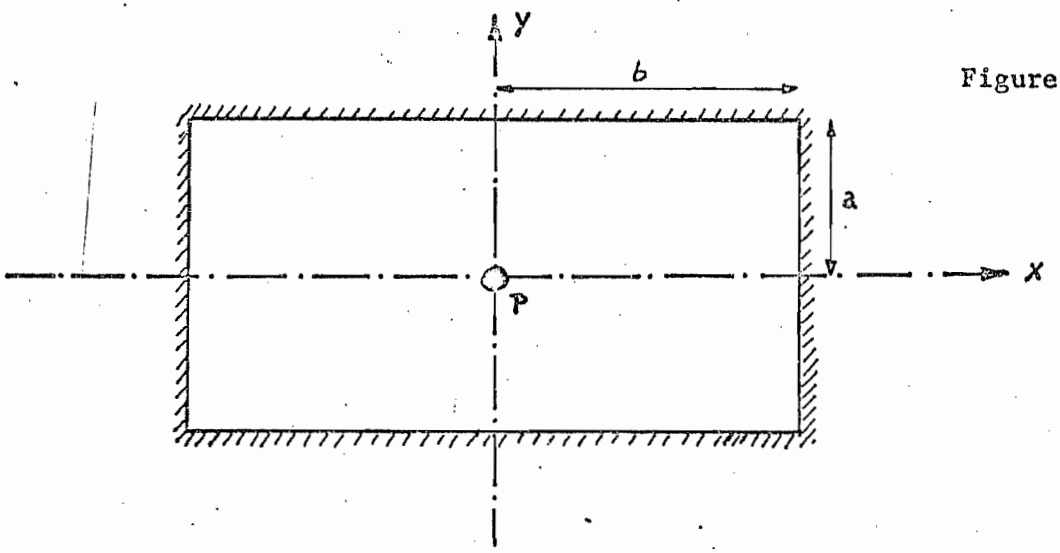

Figure 6

Case	$\frac{b}{a}$	Boundary Conditions
I	I	Simply Supported
2	2	Simply Supported
3	I	Clamped
4	2	Clamped

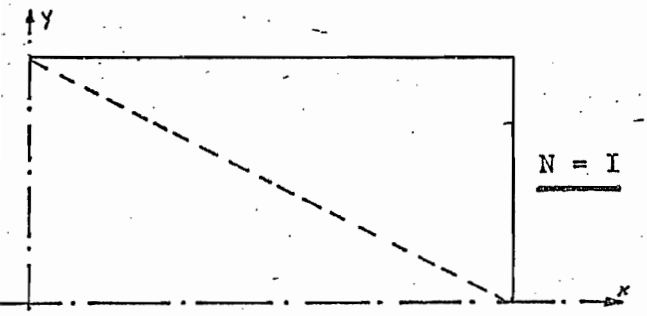

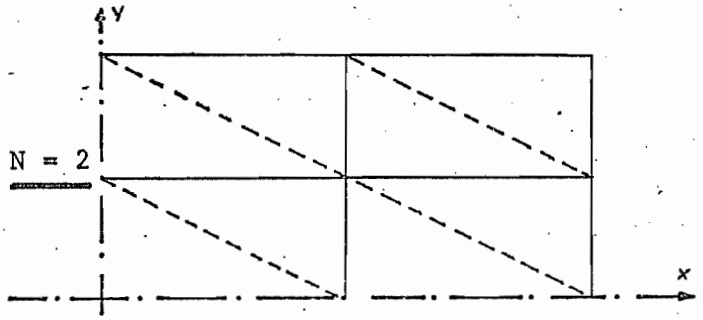

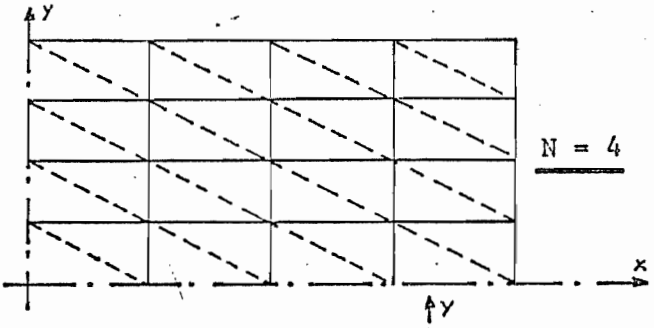

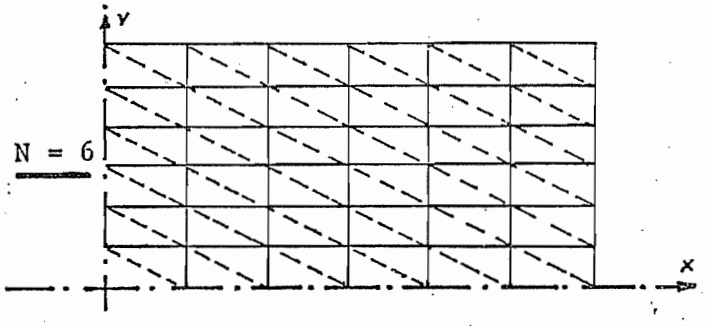

Mesh Size Number

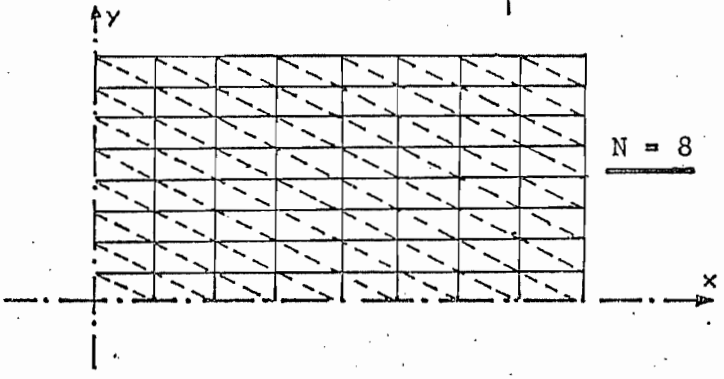

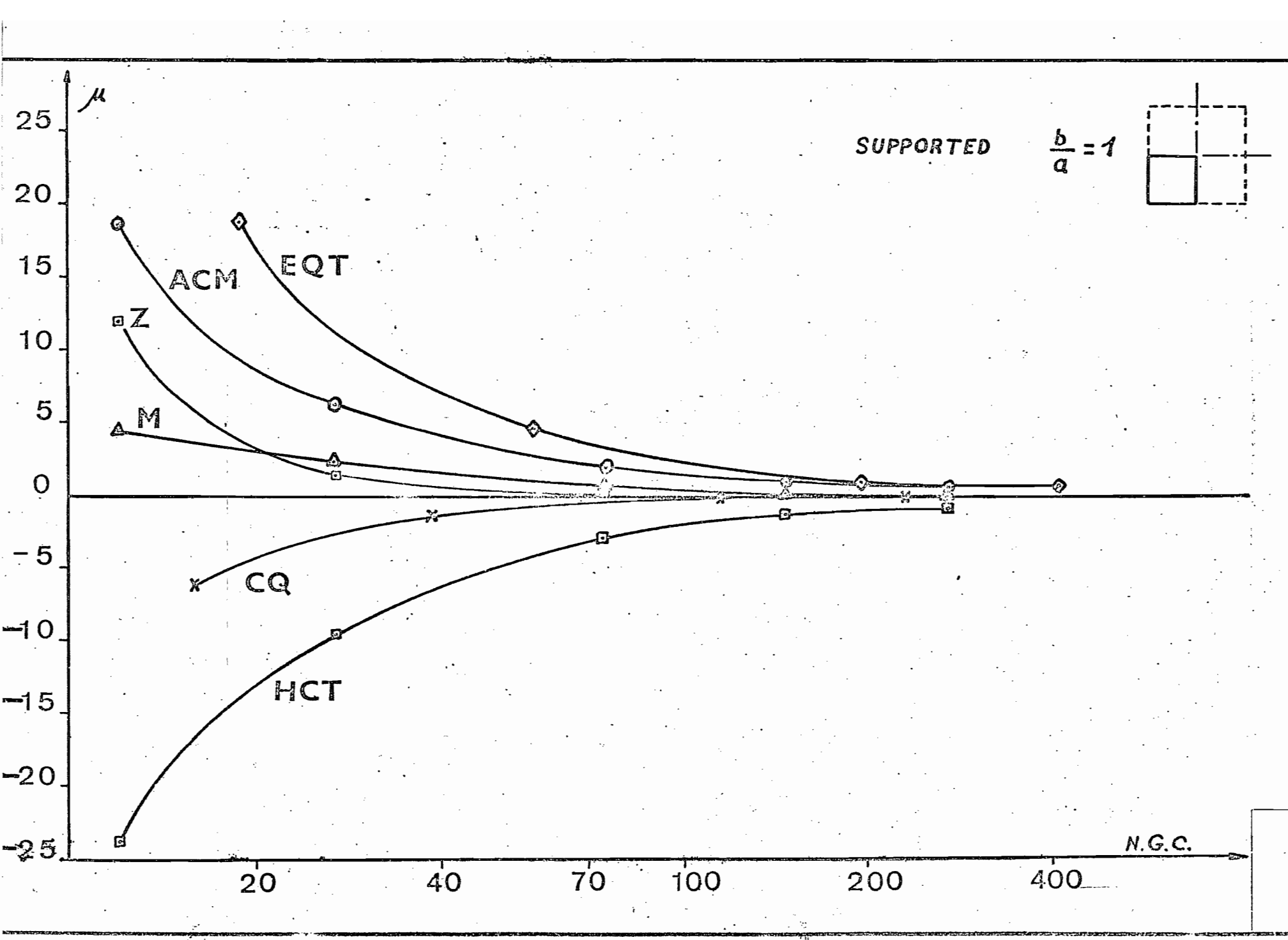
μ
25
20
15
10
5
0
-5
-10
-15
-20
-25
SUPPORTED
b/a = 1
ACM
EQT
Z
M
CQ
HCT
N.G.C.
20
40
70
100
200
400

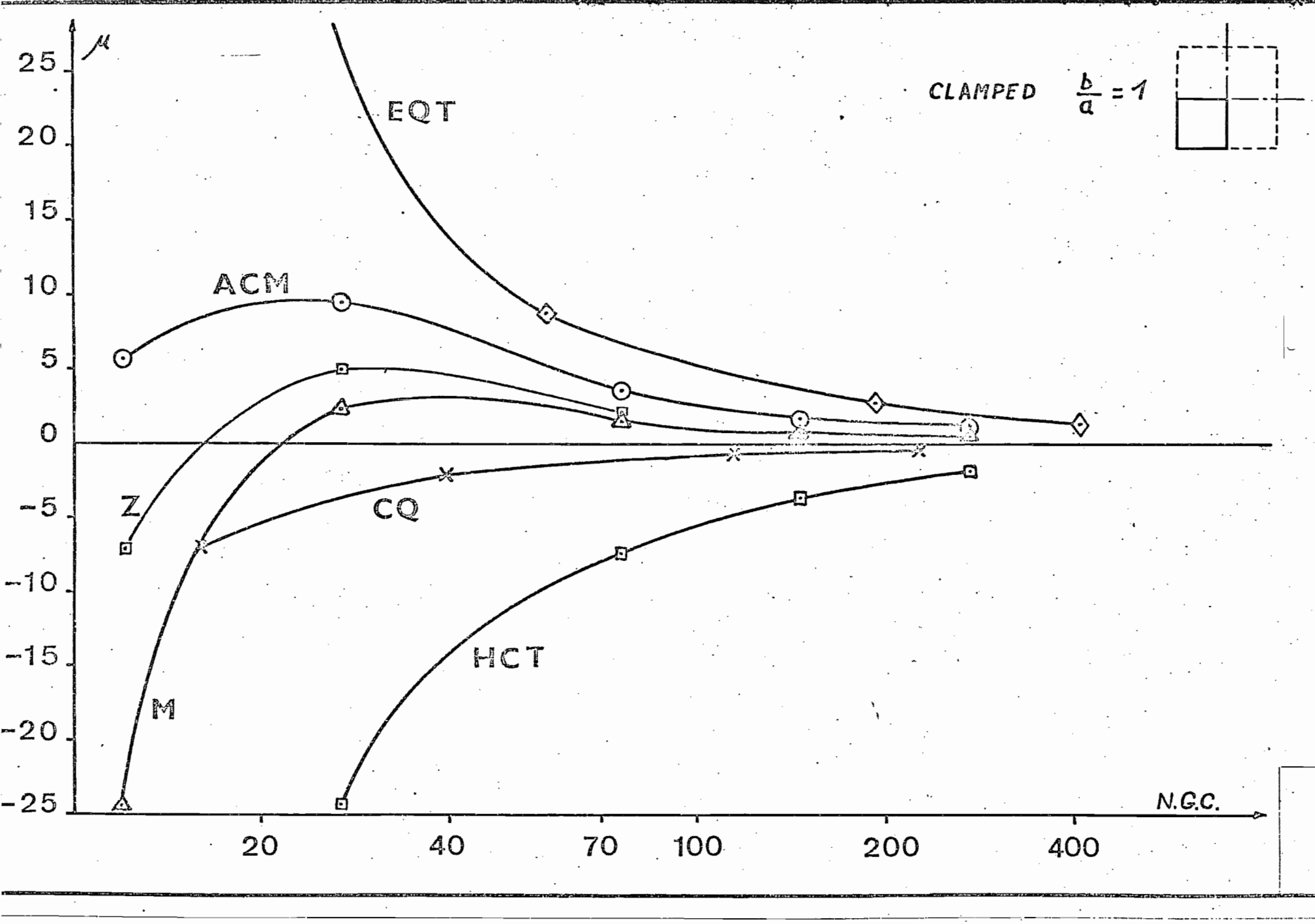
μ
25
20
15
10
5
0
-5
-10
-15
-20
-25
EQT
ACM
Z
CQ
M
HCT
CLAMPED
b/a = 1
N.G.C.
20
40
70
100
200
400

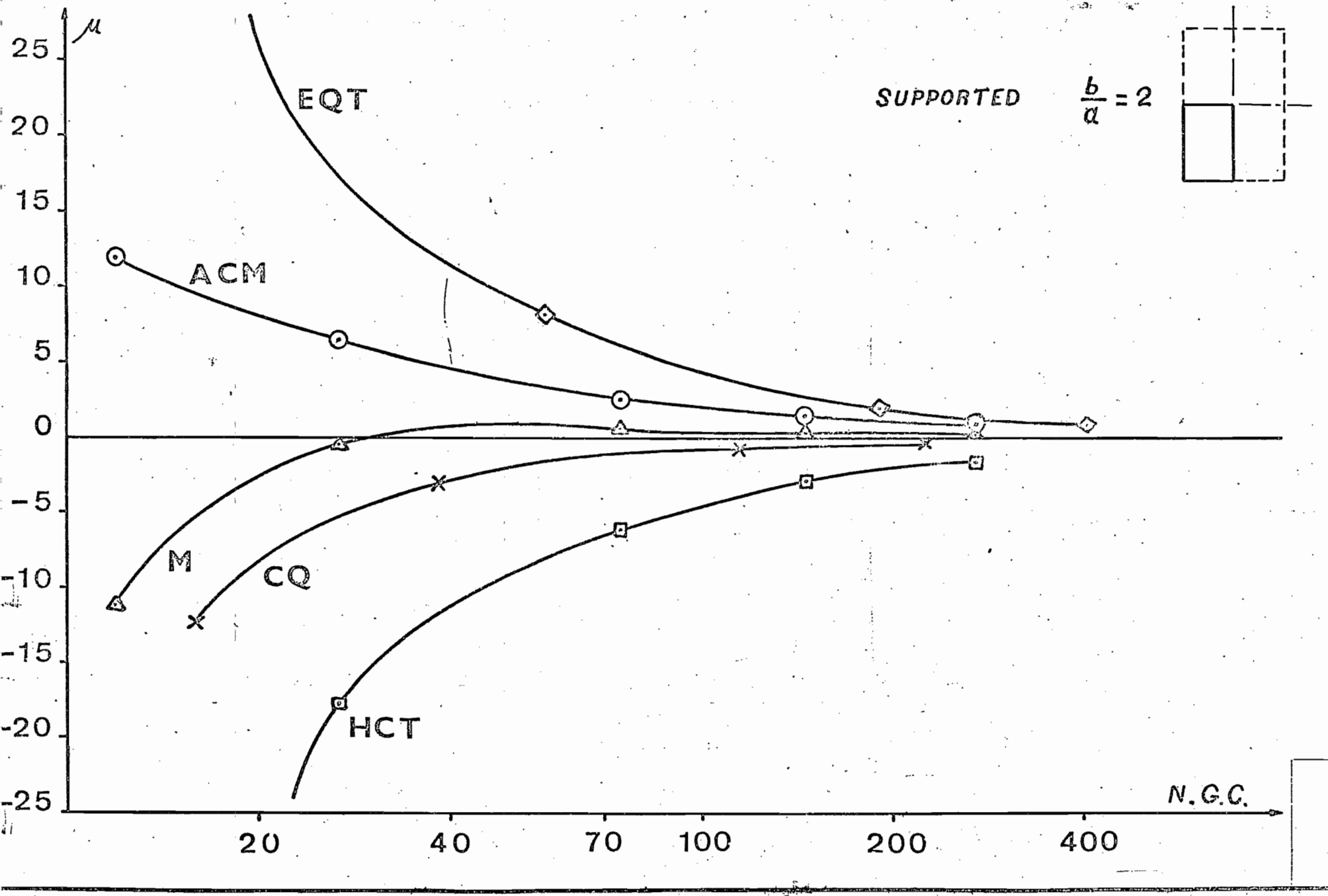
μ
25
20
15
10
5
0
-5
-10
-15
-20
-25
EQT
ACM
M
CQ
HCT
SUPPORTED
b/a = 2
N.G.C.
20
40
70
100
200
400

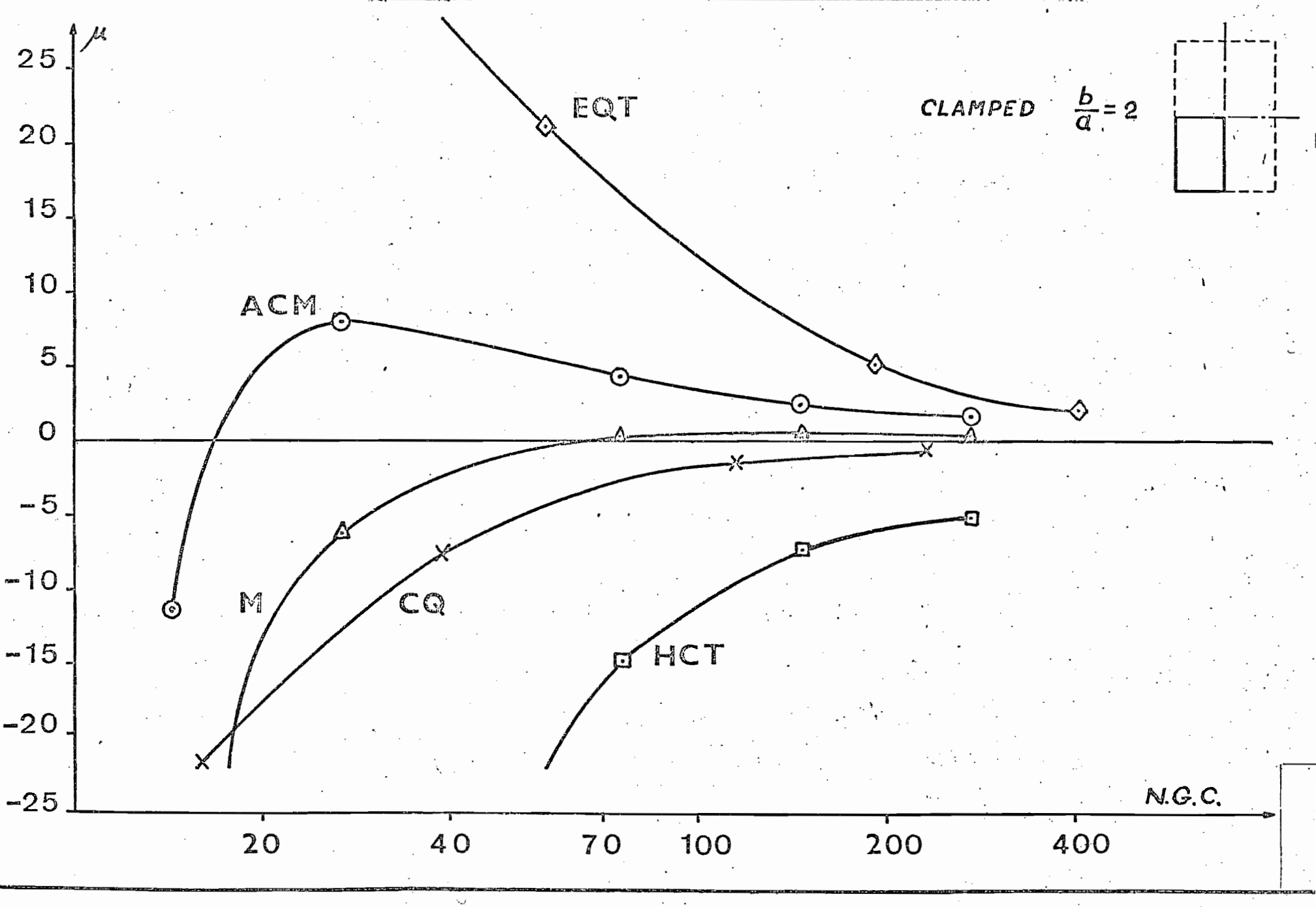
μ
25
20
15
10
5
0
-5
-10
-15
-20
-25
EQT
CLAMPED $\frac{b}{a}=2$
ACM
M
CQ
HCT
N.G.C.
20
40
70
100
200
400

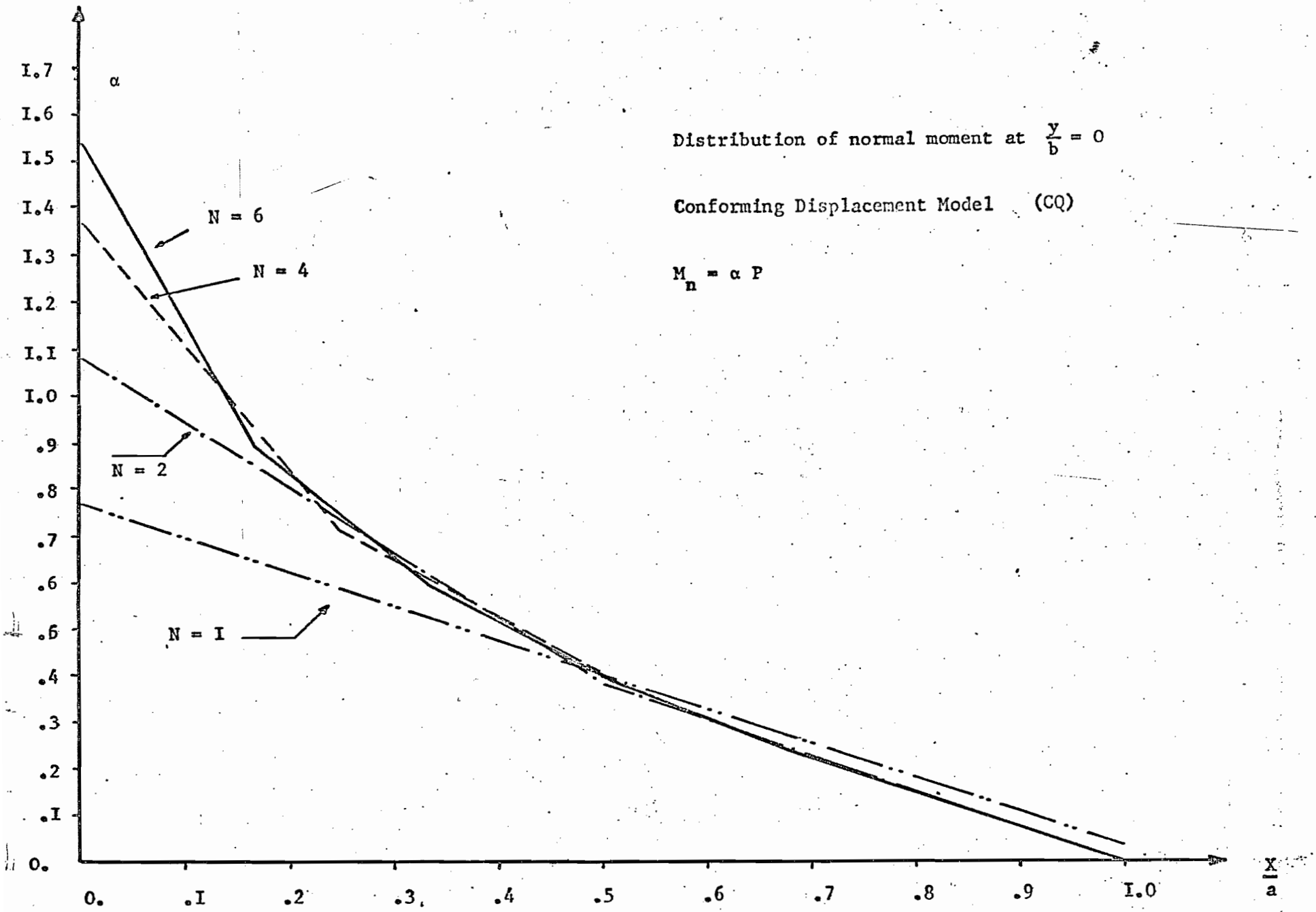
α
I.7
I.6
I.5
I.4
I.3
I.2
I.I
I.0
.9
.8
.7
.6
.5
.4
.3
.2
.I
0.
N = 6
N = 4
N = 2
N = I
Distribution of normal moment at $\frac{y}{b} = 0$
Conforming Displacement Model (CQ)
$M_n = \alpha P$
0.
.I
.2
.3
.4
.5
.6
.7
.8
.9
I.0
$\frac{x}{a}$

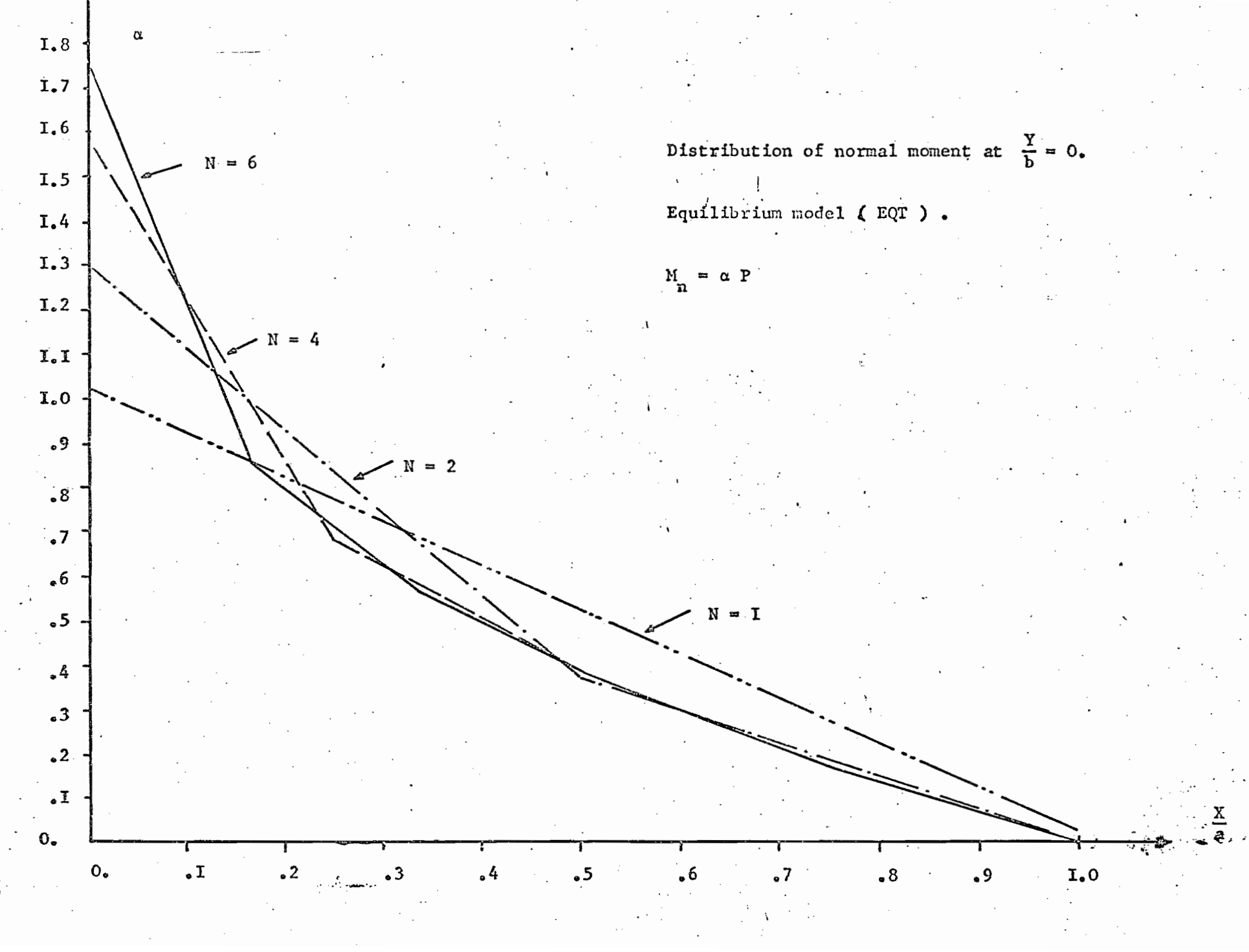
α
I.8
I.7
I.6
I.5
I.4
I.3
I.2
I.I
I.0
.9
.8
.7
.6
.5
.4
.3
.2
.I
0.
N = 6
N = 4
N = 2
N = I
Distribution of normal moment at Y/b = 0.
Equilibrium model (EQT) .
$M_n = \alpha P$
X/a
0.
.I
.2
.3
.4
.5
.6
.7
.8
.9
I.0

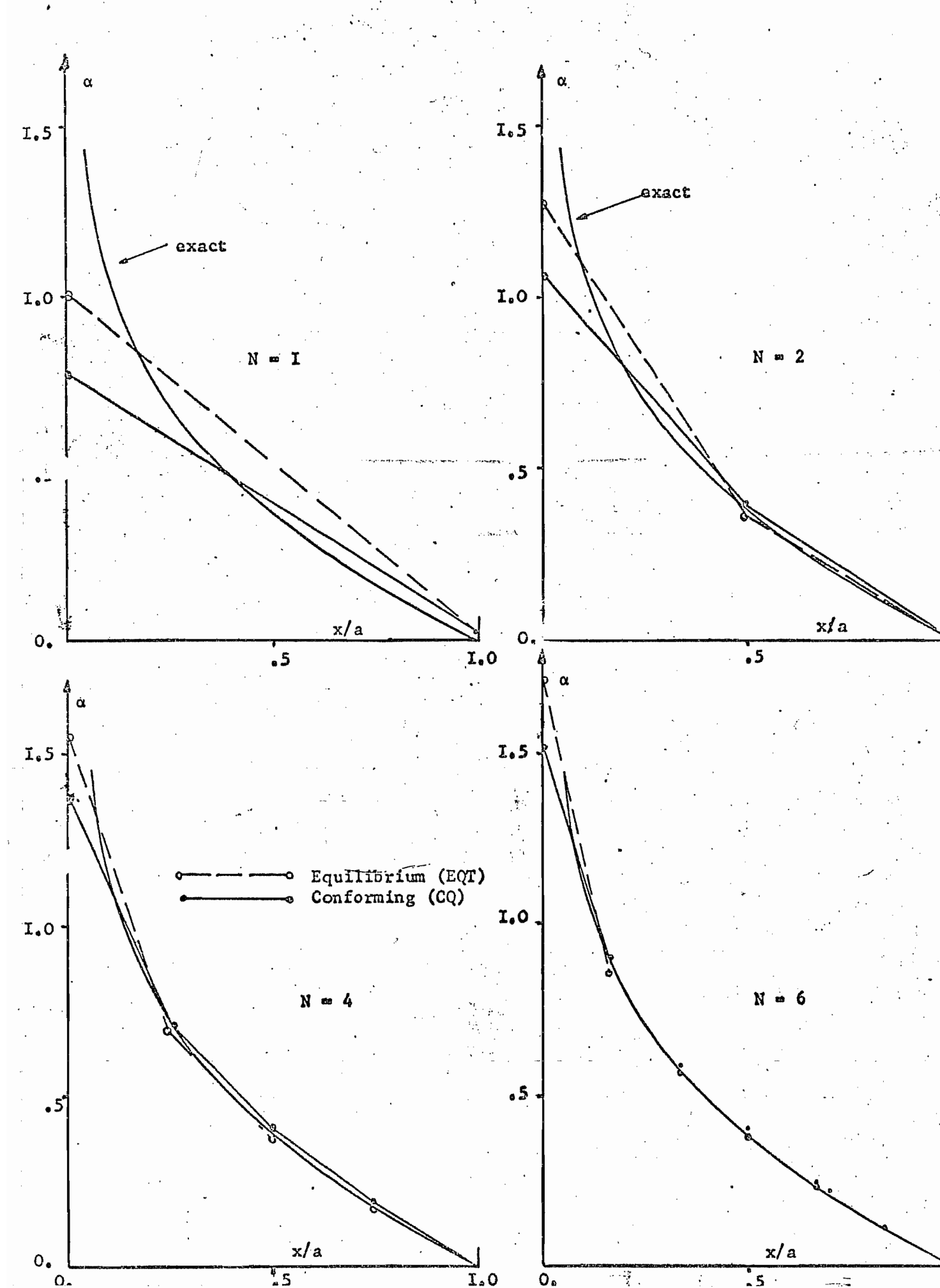
α
I.5
I.0
.5
0.
exact
N = I
x/a
.5
I.0
α
I.5
I.0
.5
0.
exact
N = 2
x/a
.5
α
I.5
I.0
.5
0.
Equilibrium (EQT)
Conforming (CQ)
N = 4
x/a
0.
.5
I.0
α
I.5
I.0
.5
N = 6
x/a
0.
.5